



RESEARCH ARTICLE

PEROVSKITE SOLAR CELLS TECHNOLOGY: A REVIEW OF ADVANCES IN CONVERSION EFFICIENCY, STABILITY AND ELABORATION TECHNIQUES ENHANCEMENT

Anateessodossomondom¹, Kata. N'detigma^{1,2} and Samah Hodo-Abalo¹

1. La MERE, Laboratoire Matériaux, Energie Renouvelable et Environnement ; Kara University, Kara, Togo.
2. Laboratoire Electronique, Informatique, Télécommunication et Energies Renouvelables Gaston Berger University, Saint-Louis, Senegal.

Manuscript Info

Manuscript History

Received: 14 September 2025

Final Accepted: 16 October 2025

Published: November 2025

Key words:-

Perovskite solar cells, efficiency, stability, elaboration techniques.

Abstract

Perovskite solar cells (PSCs) have achieved an exceptional conversion efficiency of 26.7% in 2024, just 0.6% of the record set by competing silicon technology. Improvements in elaboration techniques and the outstanding optoelectronic properties of perovskite have enabled this significant progress. This review focuses on the performance of PSCs in terms of conversion efficiency, stability and elaboration techniques. Based on a dye-sensitised solar cell, PSCs have benefitted from molecular engineering, interfacial engineering, solvent engineering and optimised elaboration methods. Difficulties such as toxicity, stability and scalability are increasingly overcome. The gradual advance in stability, highlighted by the retention of conversion efficiency ($\geq 90\%$ initial PCE) after more than 1000 hours, is a hopeful sign that the technology is reaching maturity. Despite these lightning advances in the organometallic perovskite family, efforts must be made to achieve high efficiency, lower cost and, most of all, highly stable cells for future commercialisation. Inorganic perovskites, however, are more stable despite their lower conversion efficiency yet continue to progress towards higher performance. Quantum dots (QDs) have been widely exploited to control the optoelectronic properties of cells and improve their stability to approach the theoretical efficiency limit of the technology.

"© 2025 by the Author(s). Published by IJAR under CC BY 4.0. Unrestricted use allowed with credit to the author."

Introduction:-

PSCs are one of the most promising third-generation technologies and the main competitor to silicon technology [1]. It is a low-cost alternative to conventional silicon cells due to its wide range of applications, including tandem solar cells, building-integrated photovoltaics, aerospace applications, energy storage systems such as batteries and supercapacitors, and photocatalysis [2]. These advantages derive particularly from its optoelectronic and electrical properties, such as high absorption coefficients, bandgap compatibility, low exciton binding energy, ambipolar transport characteristics, high charge carrier mobility, long carrier lifetime, carrier diffusion length in the micrometre

Corresponding Author:- Kata. N'detigma

Address:- La MERE, Laboratoire Matériaux, Energie Renouvelable et Environnement ; Kara University, Kara, Togo. 2. Laboratoire Electronique, Informatique, Télécommunication et Energies Renouvelables Gaston Berger University, Saint-Louis, Senegal.

range and high defect tolerance [1–3]. These exotic electronic and optoelectronic properties have caught the attention of photovoltaics, optoelectronics and electronics fields. These cells are economically more viable since they are easier to manufacture and available in larger quantities. This synthesis focuses on the evolution of conversion efficiency and stability since the introduction of this cell, as well as on the different families of PSCs and their production techniques.

Methodology:-

This systematic review was conducted following a rigorous methodology to analyse the evolution of perovskite solar cells. The literature search was performed primarily using the Web of Science and Scopus databases, covering the period from 2009 to 2024, and combined key concepts including perovskite solar cells, efficiency, stability, and fabrication techniques. The selection process prioritised original articles with complete experimental data and certified efficiency, while excluding purely theoretical studies and non-photovoltaic applications.

Progress in conversion efficiency and stability

Kojima et al. (2009) first integrated perovskites (MAPbI₃, MAPbBr₃) into dye-sensitised solar cells (DSSCs) to address organic DSSCs' narrow bandgap, achieving PCEs of 3.83% and 3.13%, respectively. However, low external quantum efficiency (~50%) and poor quantum dot adsorption on TiO₂ limited performance [4]. To overcome these issues, Im et al. treated TiO₂ surface, a charge transport material (CTM), with Pb(NO₃)₂ improving PCE to 6.56% but stability remained poor (80% PCE loss after 10 min) [5]. By replacing liquid electrolytes with CsSnI₃ as hole transport material (HTL), a great stability was achieved, boosting PCE to 8.5% [6]. During the same year, a similar treatment using 2,2',7,7'-tetrakis-(N,N-di-p-methoxyphenylamine)-9,9-spirobifluorene (spiro-MeOTAD) as HTL and MAPbI₃ absorber help achieving 9.7% PCE with 500-hour air stability [7]. Surface management proposed by Lee et al. using insulating mesoporous alumina (m-Al₂O₃), easier best charge extraction in perovskites absorber to reach 10.9% of PCE [8]. With a similar process, Ball et al. achieved 12.3% PCE combining compact layer TiO₂ (c-TiO₂) in TiO₂/Al₂O₃/perovskite stack benefiting of the low temperature possessing of m-Al₂O₃ and great charge separation ability of c-TiO₂[9]. Another CTM, ZnO as electron transport layer (ETL) for flexible cells proposed by D. Liu et al. make devices reach 15.7% PCE [10]. Absorber engineering including, solvent, crystallisation and post-processing [11], composition [12], deposition process [13], interface and heterojunction [14], morphology and texture [15], ... are among others techniques widely used to improve cell performance. Band gap engineering perform by a partial substitution of iodine by bromine (MAPbI_{3-x}Br_x) improved the quantum efficiency through lattice parameter shrinking towards the cubic, which is the most stable perovskite phase and ideal band gap [16]. Absorber engineering perform by Im et al. (2014) optimised MAPbI₃ cuboid size exploiting multi reflexion, helping to improve PCE to 17.1% [17].

This is possible by controlling concentration of methylammonium iodide (MAI) and the loading time. As result, similar to mesoporous structure for high surface charge extraction, cuboids offer high surface light absorption. The key role that interfaces plays in solar cell performance, especially perovskite, makes them one of the most widely used ways to improve performance in the literature. since 2014, Zhou et al., proposed ethoxylated polyethyleneimine (PEIE)-treatment of ITO modifying work function and TiO₂-dope with yttrium reducing conduction band minimum and cobalt and lithium co-dope Spiro-MeOTAD favouring best band energy alignment. With suppressed recombination at interfaces, a high efficiency of 19.3% is achieved without any information about the stability [18]. A very stable and negligible hysteresis cells (FAPbI₃) were achieved by Yang et al., reaching a PCE of 20.11%. DMSO solvent engineering, based on PbI₂-DMSO, an intermediate phase with excellent molecular exchange capacity that retards rapid crystal growth, it promote the formation of a stable crystalline phase of FAPbI₃[19]. In 2017, a systematically investigation on two-step FAI chemical deposition process on the PbI₂ showed how a few residual PbI₂ content affects cell performance, hysteresis, and stability. Optimal conditions (1300 rpm spin speed) yielded minimal hysteresis (1.5%) and peak efficiency of 21.6% (certified 20.9%) for 0.0737 cm² cells[20]. Employed poly(3-hexylthiophene) (P3HT) as HTL, a dopant-free, cost-effective, and easily synthesised material, gives 23.3% PCE.

However, unlike PTAA and spiro-MeOTAD, P3HT suffers from non-radiative recombination at the perovskite interface, typically limiting open-circuit voltage. To addressed this issue a bilayer architecture with an ultrafine wide bandgap n-hexyl trimethyl ammonium bromide and ordinary perovskite halide. This approach helps to achieved ~1.15 V open-circuit voltage, demonstrating effective suppression of interfacial non-radiative recombination. The resulting cells exhibited minimal hysteresis and excellent stability, maintaining 80% efficiency after 1008 hours without encapsulation[21]. Similarly, Jeong et al. 2020 focus on optimising spiro-MeOTAD using its analogous

isomers spiro-mF and spiro-oF. These should lower energy levels and improve molecular packing and hydrophobicity thanks to the dipole induced along the C-F bond. An efficiency of 24.82% is reported, with only 0.3V loss across the gap. This cell has a stability of 500 hours with a retention of more than 87% of the initial PCE [22]. Although this cell has good efficiency, stability was a concern when considering the application. Regarding PCE, this cell holds the conversion efficiency record of 25.5% in 2020 and 25.7% in 2022. The biannual publication by Green et al. gives a maximum efficiency of 26.7% in 2024 [23]; however, no information about stability has been given. Fig.1.a. illustrates progress in PCEs with a steady increase in conversion efficiency between 2009 and 2024.

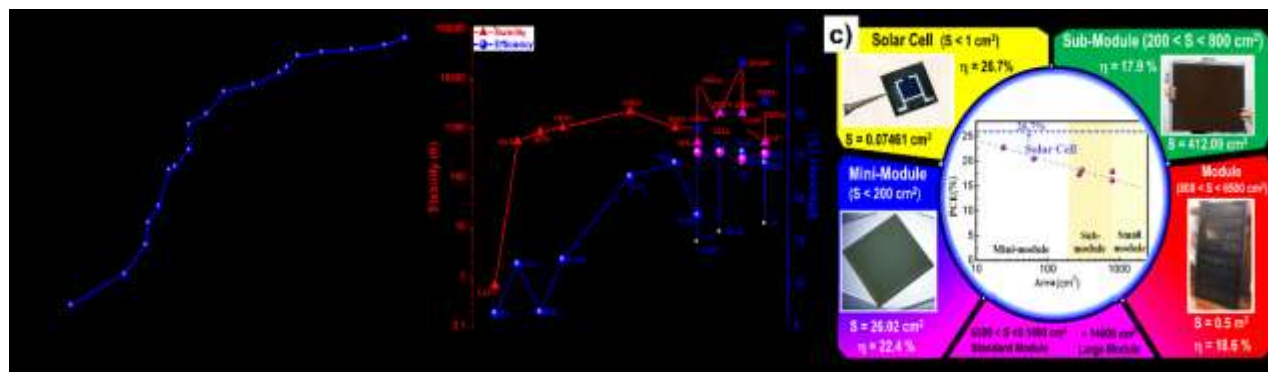


Fig. 1. a) PCEs of progression of PSCs, b) Coupled evolution of stabilisation duration and efficiency of some PSCs, c) Illustration of decreasing PCEs with increasing area

With PCE close to silicon (27.3%), long-term stability remains the limit to commercialising PSCs. Works are now focusing on the stability of PSCs through the application of passivation materials [24, 25]. The instability previously attributed to hysteresis has now been shown to be related to ion migration. According to Tumen-Ulzii et al., the source of hysteresis is the accumulation of positive ions at the ETL interface due to OH⁻ ions remaining on the cathode. Hysteresis has been suppressed using C60 pyrrolidine tris acid, a fullerene derivative (C60), to deactivate these OH⁻ groups. This treatment suppressed the hysteresis and increased cell stability [26]. Another way to improve stability is the application of surfactants with polar heads and long hydrophobic twin tails. Ren et al., through this application, improved several properties related to controlling crystallisation kinetics, especially in fully carbon-coated perovskites [27]. Since 2019, tremendous progress has been reported, showing the beginning of the mastery of the conversion efficiency and stability dilemma.

Encapsulation-free cells with a stability of 1000 to 20000 hours and an average retention of 90% of their initial conversion efficiency are reported [22, 28–31]. The average conversion efficiency of these cells is around 25%. Fig.1.b. shows the chronological development of some cells since 2012. This figure shows a significant gap between conversion efficiency and stability duration through 2019. This gap has gradually narrowed, indicating that the technology is beginning to be mastered. Stability results are increasingly encouraging, underscoring the mastery of stability. Another difficulty that needs to be overcome before perovskite technology can be commercialised is the significant decrease in conversion efficiency with increasing surface area, as shown in several studies [29, 32, 33]. Lee et al. showed in 2020 that two of the three challenges, namely the toxicity of Pb or Cs and the stability that perovskite would have to overcome to be commercialised, have been met, leaving only the control of the unfavourable surface area to PCE [34]. Fig.1.a. shows the surface area classification of perovskite-based photovoltaic devices, with the cell as the reference. The conversion efficiency decreases with increasing surface area. However, it is exciting to note that several studies have already been carried out on field tests of mini-modules or modules and that the results of these tests reveal crucial information, as well as hopes for commercialisation [35, 36]

Perovskite technology:

The breakthrough in PSC technology since 2009 by Kojima and colleagues [4] has been the catalyst for an explosion of research into improving the performance of these cells. Over the past decade, the focus has been on performance, which has increased by a factor of 7.03 compared to the efficiency of the first cell of 3.8%, now reaching an efficiency of 26.7%. Replacing the liquid electrolyte with spiro-MeOTAD led to an efficiency that over doubled (9.7%), attracting more attention than ever in the field [7]. PSCs, with a certified PCE of 26.7% in 2024 [37], efforts are focused entirely on the stability of volatile organic compounds and large-scale production, which are currently

the main obstacles to the commercialisation of this technology [3, 32, 33, 38]. In research of alternatives to overcome this stability problem, several perovskite structures have emerged, mainly due to the substitutability of most of the perovskite components.

Perovskite structure :

Perovskite is a material based on metallic, organic and inorganic halides that groups a set of materials whose structure is inspired by calcium titanate CaTiO_3 . The family general formula is ABX_3 where A is usually an inorganic or organic monovalent cation while B is a divalent. In a much wider context, A and B can be replaced by any metal or semi-metal in the periodic table [39]. Thus, these different structures can be crossed with double perovskites [40] or those widely used in applications of electroluminescent diodes [41], photoelectrochemical cells [42][43], and ferromagnetic [44]. X of the formula ABX_3 is an oxygen atom for oxides but a halogen, sulphide and nitride in other cases. In the case of solar cells, B is often represented by Pb^{2+} and Sn^{2+} , while A is composed of Cs^+ , methylammonium, and formamidinium, which are widely used.

These include MAPbI_3 ($\text{CH}_3\text{NH}_3\text{PbI}_3$), formamidinium lead iodide $\text{HC}(\text{NH}_2)_2\text{PbI}_3$, FAPbI_3 . Based on the general formula, the arrangement of atoms within the crystalline grid, variations in symmetry and distortions of the octahedron of the X elements lead to cubic, tetrahedral and orthorhombic networks [45]. Depending on the crystallographic structure and network composition, the material properties will change slightly according to the desired application [39]. Knowledge of the structure helps to understand these materials' properties and potential applications. The chemical nature and the electronic structure of the constituents, the geometry of the network, confer to this family of materials particular properties such as dielectric properties, optical properties, ferroelectricity, superconductivity, piezoelectric, multiferroicity, colossal magnetoresistance and catalytic activity [44]. A complete or partial substitution of a component can act as a dope, modifying the electronic structure [46]. This action can also change the network parameter towards a more stable structure [41, 46].

Thus, perovskites can be classified according to the spatial disposition of structure as zero dimension (0D), mainly QDs and nanoparticles, and one-dimension perovskites (1D), including nanowires and nanorods [46]. The two-dimensional (2D) perovskites are also distinguished in nanoplates and nanosheets, and finally those in 3D. Taken individually or in combination, these different forms have been prepared and applied as an absorbent layer and sometimes as a passivation layer [47]. 3D perovskite is the most suitable material for solar cells due to its cubic structure. The vertices of this structure are occupied by monovalent cations (A), while an octahedral site in the cube's centre hosts a divalent cation (B). This octahedral site, whose vertices carry halogens (X), is located in the centre of the faces of the cube. Finally, this structure forms a complex network, offers great flexibility for manipulation at will and abundance on Earth.

Perovskite Family :

Organometallic-base Perovskite

Methylammonium lead iodide (MAPbI_3) is undoubtedly one of the most primitive and ideal models for the perovskite family of solar cells, prized for its exceptional properties: high electron ($7000\text{-}30000\text{ cm}^2\text{V}^{-1}\text{s}^{-1}$) and hole ($1500\text{-}5500\text{ cm}^2\text{V}^{-1}\text{s}^{-1}$) mobility, and an ideal $\sim 1.5\text{ eV}$ bandgap [28]. However, MAPbI_3 -based cells face significant challenges: toxicity due to lead, which is hard to replace effectively [49, 50], interface defects that cause non-radiative recombination and harming performance [51, 52]. Finally, instability under humidity, heat, and UV-light, hindering commercialisation [53]. A key issue is the rapid crystallisation process used to make these films, which promotes grain boundaries. These boundaries lower device performance by enabling non-radiative recombination, ion migration, and loss of volatile species [53].

This problematic nucleation stems from the colloidal nature of the precursor solution, caused by the low solubility of PbI_2 compared to MAI. Using specific solvents like N, N-dimethylformamide (DMF), γ -butyrolactone (GBL), dimethylsulfoxide (DMSO), 2-methoxyethanol (2-ME), acetonitrile (ACN), N,N-dimethylacetamide (DMAA), and N-methylformamide (NMF), and additives like MACl can reduce large colloids and inhibit Pb^0 defects formation [53]. Controlling the precursors and crystallisation, for instance within a mesoscopic $\text{TiO}_2/\text{ZrO}_2$ /carbon triple, framework, can yield highly oriented, stable films. Another promising method is inverse temperature crystallisation, which uses a heated precursor solution to dissociate complexes and grow high-quality crystals efficiently [53, 54]. Along with MAPbI_3 , FAPbI_3 is one of the most widely published organometallic perovskites. The main reason for this is its excellent stability [55, 56] with all other properties, including an ideal gap between 1.45 eV and 1.51 eV [57] and its ability to reach the theoretical efficiency limit [58]. It reaches 25.6% in 2023 [59], and this could be

due to better carrier separation, which can be attributed to the formation of large polarons that protect charges to recombination [59], thus increasing carrier lifetime and diffusion length. However, FAPbI₃ is affected by a phase transition from photoactive black (α -FAPbI₃) to non-photoactive yellow (δ -FAPbI₃) at temperatures below 150°C [60]. Therefore, it is essential to control this phase transition. By exposing FAPbI₃ to methylammonium thiocyanate vapour at 100°C, Lu et al., converted the yellow phase of FAPbI₃ into a highly crystalline black phase. The resulting cell retains this phase after 500 h at 85°C with an efficiency of 23.1%. It maintains 90% of this efficiency after 500 h under MPP irradiation with very low hysteresis, indicating low electrical charge trapping at the interfaces. [60].

Inorganic-base Perovskite:

Caesium lead bromide (CsPbBr₃) and caesium lead iodide (CsPbI₃) perovskites are the most commonly reported inorganic perovskites in the studies due to their exceptional electronic and optoelectronic properties in keeping with the perovskite family. Without encapsulation, inorganic perovskites can remain intact in humid air (90-95% relative humidity, 25°C) for over 2640 h without degradation and can withstand extreme temperatures (-22 and 100°C) [61]. CsPbI₃ and CsPbBr₃ have band gaps of 1.73 and 2.3 eV, respectively [48], which makes them good light absorbers. The main attraction of inorganic CsPbI_xBr_{3-x} perovskites (x = 0 to 3) is their superior thermal stability compared to inorganic, organic metal halide perovskites [62]. However, their PCE is low compared to organometallic lead halide perovskites. This low PCE is thought to be due to poor film quality linked to defects and trap sites, resulting in low short-circuit currents and poor phase stability.

Among these inorganic CsPbI_xBr_{3-x} perovskites, CsPbBr₃ shows better stability; however, it has a wide band gap of about 2.3 eV, which is not ideal for photovoltaic applications. CsPbI₃ and CsPbI₂Br, with relatively narrow band gaps of about 1.73 and 1.92 eV, respectively, are more suitable for solar photovoltaics. Their thermal stability decreases significantly when exposed to harsh environmental conditions such as humidity, heat, UV radiation, etc. CsPbIBr₂ has much more balanced properties, such as a band gap of 2.05 eV and phase stability, making it the most promising material for optoelectronic devices [62]. CsPbI₃ crystallises in different structures such as the orthorhombic including δ phase (Pnma) and γ phase (Pnam), the cubic α phase structure (Pm3m) and the tetragonal β phase structure (P4/mbm) [63]. The Goldschmidt tolerance factor (t) can assess the stability of perovskite crystal structures.

$$t = \frac{R_A + R_X}{\sqrt{2}(R_M + R_X)} \quad (1) \quad \mu = \frac{R_M}{R_X} \quad (2)$$

R_A and R_M are the ionic radius of the monovalent and divalent cation, respectively, and R_X is the radius of the anion. This factor reflects the degree of distortion of the perovskite. The octahedral factor (μ) indicates the occupancy of the MX₆ octahedron. The corresponding values for halogenated perovskites are 0.81 < t < 1.11 and 0.44 < μ < 0.90. In the particular case of CsPbI₃, where the smaller atomic radius of Cs⁺ with t = 0.8472 is a bit extreme, CsPbI₃ readily transforms into non-photo-active orthorhombic δ -CsPbI₃ under thermal and moisture stress. Black (α -phase) at 360°C, after cooling to beta-phase at 260°C, then gamma-phase at 170°C, all yellow phases. Producing CsPbI₃ cells with high phase stability at room temperature is a challenge. Efforts such as removing MA from Cs_xMA_{1-x}PbI₃, the first technique used for this technology, formed the yellow phase with almost zero yields [63, 64]. Hydroiodic acid (HI), used as an additive during the one-step deposition, significantly reduces the crystallisation temperature of the alpha phase with an absorption edge at 717 nm, albeit with a very low PCEs of 2.3% [65].

This was adopted by several authors with hydroiodic acid derivatives such as HPbI₃ and HPbI_{3+x}. However, studies showed that these acids would react with N, N-dimethylformamide (DMF) to form formic acid and dimethylamine (DMA) [63, 66]. The proper additive would be dimethylamine iodide (DMAI), which would have formed a mixed perovskite Cs_xDMA_{1-x}PbI₃ with CsPbI₃ [63, 67, 68]. However, the UV-visible absorption spectrum shows no difference in the Cs_xDMA_{1-x}PbI₃ content for different DMA contents in the samples. Wang et al. showed that DMAI could manipulate crystallisation via the DMAPbI₃ intermediate phase. This phase would facilitate the formation of pure α -CsPbI₃ crystals of good quality after annealing [69]. The volatility of DMAI enables this intramolecular exchange. Many other volatile organic cations, such as MA⁺ and FA⁺, are used, as well as methylamine acetate (MAAc) and formamidinium acetate (FAAc). Recently, dimethylamine acetate (DMAAc) has been used both as a solvent for precursor solutions and as a regulator of the CsPbI₃ film phase conversion process, resulting in efficiencies greater than 21% [70]. The effect of organic cations is essential for simple fabrication techniques of CsPbI₃PSCs, and exciting clues are emerging to explain the underlying mechanism, which is currently poorly understood. Organic compounds with well-chosen precursors such as CsI, PbAc₂·3H₂O and phenylethylammonium

iodide (PEAI) or CsI, PbI₂, oleylamine and acetic acid have led to the alpha phase of CsPbI₃ at annealing temperatures around 120°C [71]. Ye et al. succeeded in stabilising γ -CsPbI₃ by using excess lead acetate Pb(OAc)₂ to form 2D perovskites employing phenylethylammonium iodide, which effectively suppressed recombination in γ -CsPbI₃. In this way, they obtained a cell that maintained 95% of its PCE [72]. Several techniques such as full or partial halogen and divalent cation substitution [73], indium (InI₃) bismuth (BiI₃) doping [74, 75], surface treatment [73], and precursor engineering have been developed to slow the degradation of the black phase to the yellow phase. Perovskite-based QDs offer a promising path to improved stability. These nanoscale crystals benefit from unique properties like multiple exciton generation (MEG), which can help efficiencies beyond the Shockley-Queisser limit and turnability of optoelectronics propriety via quantum confinement [76, 77]. Among them, inorganic QD-CsPbI₃ has emerged as a leading material, achieving 16.53% efficiency [78]. It exploits high surface tension nanoscale to exhibit exceptional proprieties: narrow photoluminescence, high carrier mobility and visible light absorption. Crucially, it demonstrates excellent defect tolerance, minimising non-radiative recombination despite high defect densities. A key advantage over bulk perovskites is its suitability for large-area, printable fabrication, as it eliminates the need for precise simultaneous control of crystallinity and morphology during film deposition.

Perovskite solar cell elaboration techniques:

A thin film photovoltaic solar cell's electrical, electronic and optical performance highly depends on stoichiometry, crystallographic phases, grain structure, etc. These properties can only be achieved by controlling precursors preparation and individual layers. The deposition technique, the choice of precursors and their nature, additives, processing conditions, etc., are among the factors that allow the preparation to be controlled [79]. Several deposition techniques are used, including dip coating, thermal evaporation, spin coating, electrodeposition, doctor blade, and ink-jet printing.

Precursor preparation:

Perovskite precursors based on organic halides such as methylammonium iodide and formamidinium iodide, inorganic halides (CsI) and lead salts (PbI₂, PbBr₂ or PbCl₂) with molar ratio of x:y (organic/inorganic halides: lead salts) are used to prepare the perovskites MAPbI₃, FAPbI₃, CsPbI₃ and their mixtures. These precursors are dissolved in highly polar, often organic, solvents such DMF, GBL, NMP or DMSO [79]. By exploiting these different types of precursors mentioned, and based on the general composition of ABX₃ perovskites, various mixed structures with monovalent and divalent cations, respectively A and B and halogens X are synthesised in studies [79–81]. Examples include mixed perovskites with organic cations MA_x/FA_{1-x} and halogen mixtures I_x/Br_{1-x}, I_x/Cl_{1-x} or Br_x/Cl_{1-x}, organic-inorganic complexes such as (Cs_{1-x-y}/FA_x/MA_y)Pb(I_{1-a}/Br_a) [81] or (Rb_{1-x-y-z}/Cs_x/FA_y/MA_z)Pb(I_{1-a}/Br_a). These complex systems enable more stable devices indicating layer quality: morphology, grain size and crystallinity [81, 82]. Once the precursors have been prepared, they are deposited on substrates using various techniques described in the deposition techniques section.

Deposition techniques :

Thin-film cells, including perovskite, are manufactured using various techniques. The choice of technique is essentially based on two main criteria: the quality of the deposited layers and the cost of the method. In addition, industrial production criteria can be taken into account. However, these criteria are less critical for silicon, which is already mature, than for perovskite, which is still at the laboratory stage.

Vacuum thermal evaporation deposition:

Thermal evaporation is a physical vapor deposition (PVD) technique that deposits thin film devices. It is commonly used in microelectronics. It involves the "Joule effect" heating of a material placed in a tungsten crucible to reach the vaporisation phase. In a vacuum or inert enclosure, the vapor is deposited by condensation onto a temperature-controlled substrate. The substrate is often rotated to improve the homogeneity of the deposited layers, which is quite different from the spin coating (see Fig.2.1.a). The precision of vacuum thermal evaporation makes it one of the best deposition techniques for film quality control. Vacuum thermal evaporation has the advantage of not using solvents, precise control of film thickness, and large-scale production capability [83]. In the specific case of PSCs, thermal evaporation is carried out with one, two or even three sources, depending on whether several solid precursors (powders) are used (Fig.2.1) [84]. Evaporation can be simultaneous or sequential. The deposited perovskite layer is strongly influenced by the temperature in the chamber, the substrate temperature, the evaporation rate, and even the molecular weight of the precursor. As the number of sources increases, managing the composition of mixed perovskites becomes more challenging [84]. Although it is a very high-level deposition method, it still has some progress in compositional control compared to spin coating. There is continuous progress in cell efficiency

using this technique with PCE reaching 25.16% in 2025[85]. Thermal evaporation is coupled with spin coating for specific treatments requiring very high quality of the layer, as in the case of Li et al. They deposited PbBr_2 and other layers by spin coating and the CsBr_2 solution by thermal evaporation. With this method, devices maintained 80% PCE of its initial efficiency for 2160 hours at a relative humidity of 80% and a temperature of 85°C. [86]. All inorganic perovskites are said to be more stable, hence their increasing interest [61]. Lossless self-assembled HTL monolayers (2PACz, MeO-2PACz and Me-4PACz) are deposited for the first time using thermal evaporation by Farag et al. These monolayers replace conventional layers such as spiro-MeOTAD. A comparison between thermal evaporation and solution deposition on the electrical parameters of the cell clearly shows the difference in performance between the two deposition methods (see Fig.2.II) [87]. Thermal evaporation allows deposition over large areas and produces high-quality devices, but it is still very expensive.

Spin-coating:

Spin coating is one of the solution coating techniques commonly used to deposit high-quality thin films on substrates. The liquid's centripetal forces and surface tension ensure a uniform coating during rotation. The centripetal force plays a crucial role and is controlled by the rotation speed of the substrate, typically more than ten (10) revolutions per second. The advantage of spin coating over other techniques is the ease, low cost and speed with which highly uniform thin films can be produced. However, spin-coating is limited to single substrates, which are also small, and a more significant proportion of the material used is lost during rotation over 90% [88], which is an obstacle to large-scale use [89]. Spin coating involves two essential steps [90]: (1) solution deposition onto the substrate, followed by high-speed spinning. The drop of solution is deposited at the centre of the substrate and begins to rotate at a constant or variable angular velocity. Initially, the substrate and the liquid may have different rotational speeds due to drag. This rotation allows the liquid to spread and be thinned after part of it has been ejected from the substrate, minimising inertial forces.

The sufficiently thin solution rotates at the same speed as the substrate. In this way, the viscous shear drag perfectly balances the rotational accelerations. Since the total velocity is constant and the viscous forces of the solution dominate its thinning behaviour, a uniform film is obtained [91]. (2) Evaporation: under the effect of centrifugal forces, the fluid continues to thin, accompanied by the evaporation of the solvent, leaving a thin layer on the substrate (see Fig.2.III). The spin-coating technique includes several deposition methods (see Fig.2.IV). One-step deposition spin-coating is the simplest, fast, and inexpensive technique [92]. MAPbI_3 colloidal solution is directly deposited on the transparent conductive oxide (TOC)/ TiO_2 substrate by spin coating and then dried at temperatures between 70 and 100°C (see Fig.2.IV. a). The heat treatment is usually performed in glove boxes where parameters such as temperature, oxygen level, humidity, and annealing time are controlled [81]. This process produces perovskite thin films with good crystallinities and morphologies.

However, the quality is often not as desired and is accompanied by pinholes [92]. For multi-cation perovskites, an additional "quenching" step in the one-step deposition process may be indispensable to obtain uniform, dense, and highly crystalline thin films (see Fig.2.IV.b). This is done by adding a few μL of an antisolvent a few seconds before the spin-coating process ends [81]. Two-step deposition solves problems encountered in the one-step process (see Fig.2.IV.c). In this method, PbI_2 solution is first deposited after dissolution in DMF reacting strongly with the substrate by infiltration. After that, the MAI precursor is coated on to form the MAPbI_3 perovskite film. Finally, annealing is required to remove excess organic salt (MAI) and solvent to ensure better crystallinity. The two-step process has the advantage of producing more homogeneous films, better crystallinity to improved optical and electrical performance. J-W. Lee and N-G. Park demonstrated it with PCE of 7.5% and 13.9% [93] for cells prepared in one and two steps, respectively. Spin coating is the most widely used and cost-effective deposition method; however, its limitation to small surfaces prevents its use in industrial applications. A large surface area results in non-uniform precursor distribution, which leads to poor control of perovskite nucleation and crystallisation, especially for surfaces larger than 1 cm^2 .

Dip-coating:

Widely used in both industry and research, dip-coating is a prevalent technique for depositing thin films for device development [94]. This technique consists of (1) dipping the substrate in the precursor solution, (2) leaving it there for a fixed time, and then (3) removing it with thickness control via the removal rate. These are the three basic steps of dip coating, summarised in Fig.2.V. Thickness, morphology, and film coverage on the substrate are strongly affected by immersion time, shrinkage rate, number of immersion cycles, solution density and viscosity, evaporation rate, and substrate surface [95]. Dip coating was an early technique in perovskite photovoltaics since it is

inexpensive, fast, simple, yields high-quality films, and is compatible with scalable roll-to-roll processing for flexible cells [94]. It is generally applied to perovskite technology for specific layers such as TiO_2 or MAI [96]; sometimes for all layers [97]. Moreover, it is one of the most suitable for the fiber-shaped organic solar cells [98]. The performance of cells using this dip-coating has steadily increased over time. F. Li et al., combined dip-coating with reconversion of polyammonium iodide (PAPbI_3) to MAPbI_3 to achieve PCE of 19.27% and 15.68% for areas of 0.09 cm^2 and 5 cm^2 , respectively [99]. Immersion time, annealing temperature [100], and the concentration of coating precursors are among the factors influencing the device performance [101]. Recently, Rahman et al. have shown that very low-cost and stable cells can be achieved by dip-coating using p-type Si nanowires as HTLs. These silicon nanowires are better conductors than spiro-MeOTAD and significantly improve the device efficiency (23.8%) [102]. In addition, silicon is highly resistant to water and humidity, so it was possible to stabilise the PSC without encapsulation after 1200 hours at ambient temperature while cleaning with water. Challenges like pinholes, poor thickness control, and environmental sensitivity limit the industrial use of dip-coating for high-efficiency solar cells, as they cause defects that reduce performance and stability [103].

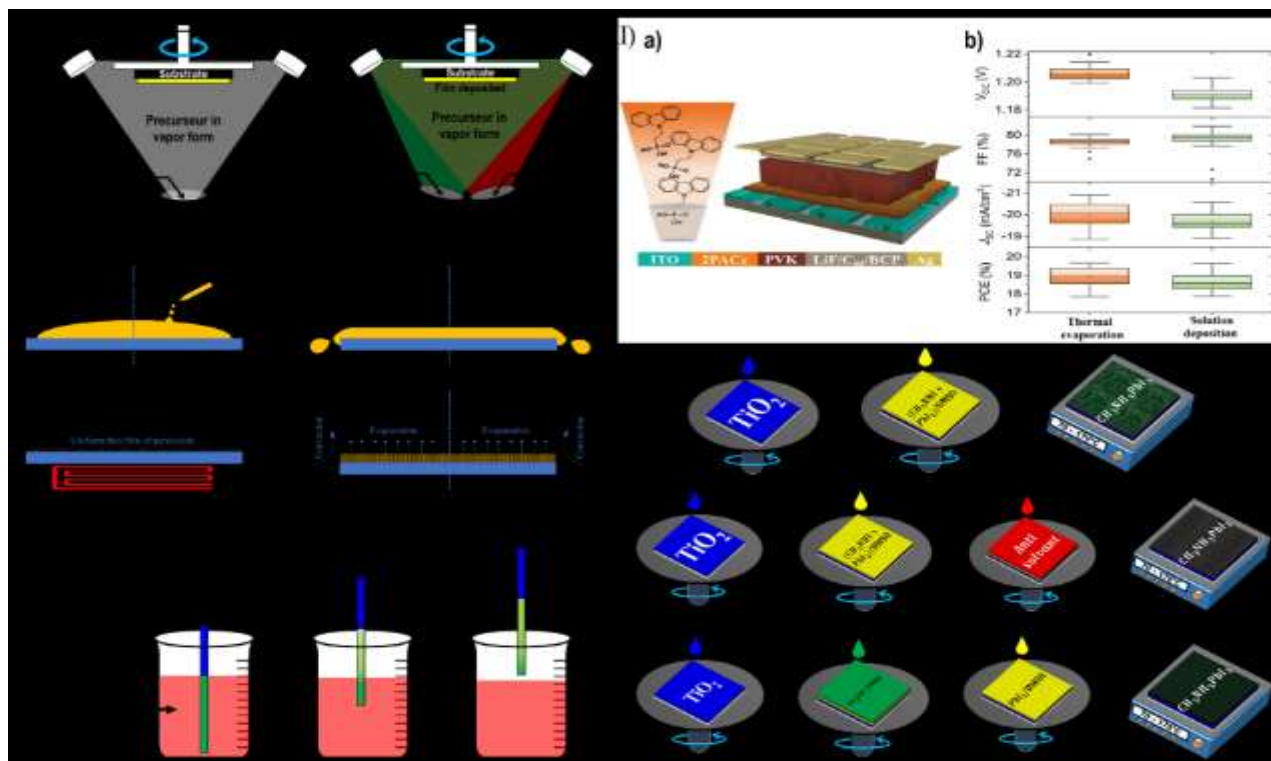


Fig. 2. I) Vacuum thermal evaporation deposition technique using: a) single source, b) dual sources; II) performance comparison between spin-coating and thermal evaporation processes for PSCs; III) spin-coating process; IV) spin-coating process: a) one-step, b) quenching step, c) two-step; V) dip coating process.

Blade coating

As a scalable deposition technique, blade coating produces large-area thin films of precise thickness. This is achieved by translating a sharp blade, set at a fixed distance from the substrate, over a coating solution that is dispensed ahead of it at a moving speed of between 0.3 and 20 cm.s^{-1} [104] (see Fig.3.I). A wet film is deposited on the substrate to be dried. Several factors generally control the thickness of the film. These include the precursor concentration, the gap between the blade and the substrate, and the blade speed moving over the substrate [105]. This technique can be adapted for continuous production with roll-to-roll equipment for flexible cells. It is very economical regarding precursor usage, with only about 5% solution loss [88]. A comparative study performed by Yang et al. showed that the gap in morphological quality between spin coating and blade coating can be narrowed. As a result, film morphology and device performance are virtually identical using both methods, as seen in Fig.3.II. Incorporating chlorine into the MAPbI_3 structure and solvent tuning in combination with an anti-solvent played a significant role in this result [106]. In this way, Yang et al. overcame the difficulty of crystallising perovskite by blade coating with rapid grain growth rates. Maximum conversion efficiencies of 18.55% and 17.33% were

achieved for devices with surface areas of 0.12 cm² and 1.2 cm², respectively. They also assembled a four-cell module with an active area of 12.6 cm² with a stabilised efficiency of 13.3%. Concerning stability, the 0.12 cm² cell retains 80% of its power after 3000 hours in ambient conditions. A promising approach that uses the blade-coating method to deposit doped perovskite without the expensive spiro-MeOTAD achieved an excellent power conversion efficiency (PCE) of 20.2% and maintained 92% of that efficiency after 500 hours in ambient conditions. This highlights a path toward both high performance and improved cost-effectiveness [104]. Utilising solvent engineering and an excess of MAI, Peng et al. fabricated good-quality PSCs under ambient humidity exceeding 40%, achieving a power conversion efficiency (PCE) of 10.92% [107]. Surfactants are used in blading to play a similar role as anti-solvents in spin coating. Surfactants with polar heads and hydrophobic twin tails are used to slow volatility and, thus, rapid crystal growth by modifying the perovskite precursor's rheological, hydrodynamic and viscoelastic properties. Controlling the kinetics of perovskite crystallisation is critical and allows optimisation of energy level alignment and neutralisation of charge defects, as shown by Ren et al., [27]. In addition, the additive 1,2-distearoyl-sn-glycero-3-phosphocholine allowed a certified record efficiency of 15.46% for fully carbon-coated perovskite-based solar modules with exceptional stability [27]. Modulation of the MAI content in perovskite by Chang et al. showed that orientation and crystallisation were significantly improved. This resulted in very high-quality films using a two-step sequential blade coating process. A high PCE of 23.14% for unencapsulated cell retained about 80% of its initial value after 1680 h at ambient conditions [108]. It is interesting to note the importance of the doctor-blading study, which opens the way for large-scale production of PSCs.

Electrodeposition:

Electrodeposition, also known as electroplating, is one of the emerging techniques for depositing large-area thin films in PSC fabrication. Its advantages are control of thin film growth, uniformity of layers, ease of implementation, flexibility and relatively low cost [109]. It is based on the principle of electrochemical reduction of perovskite precursors dissolved in a solution, allowing the deposition of perovskite films on the conductive substrate. A cathode, in this case, a conductive substrate (FTO or ITO), and a counter-electrode (anode), usually an inert electrode (platinum, graphite), is immersed in an electrolytic solution containing the PSC precursors, such as lead chloride (PbCl₂) and MAI. Applying an electrical potential between the two electrodes triggers the reduction, forming the perovskite layer on the cathode.

The exact chemical reaction depends on the specific precursors used. The deposited perovskite film can be annealed to improve crystallinity and stability. Current density, solution composition, temperature, and duration are essential parameters for optimising film growth. In 2020, Wang et al. demonstrated the critical role of these factors in the electrodeposition of CsPbBr₃ on m-TiO₂. Their work showed that current density affects pinhole density, deposition duration influences the perovskite phase formation, and applied voltage controls grain size [110]. Their study was carried out by observing the SEM images, as shown in Fig.3.III. Without encapsulation, the cell retained 99.7% of its initial efficiency after 3840 h (160 days). M. Al Katrib et al. recently obtained mixed perovskites by electrodeposition of PbI₂ by converting PbO₂ with a maximum PCE of 10%. However, the electrodeposition still needs to be improved since the current results were obtained [110, 111]. The large number of perovskite variants means that several studies must be conducted to identify the optimum current, voltage and duration values to ensure good film quality.

Ink-jet printing

Inkjet printing is a flexible, economical, automated digitisable thin film deposition technique [112]. It uses the controlled ejection of solution droplets from a print head. This allows precise droplet control and production on larger surfaces. It remains one of the most promising techniques for the efficient, scalable manufacturing of PSCs. Inkjet printing can be divided into continuous-mode inkjet and on-demand inkjet. In both cases, periodic stimulation can optimise the jet via a piezoelectric or thermal transducer [113]. Droplet manipulation inherent in fluidic interactions (viscosity, density, and surface tension), nucleation regulation, and crystallisation are key factors in the quest for deposit quality [112]. Ink engineering, printing processes, and post-deposition treatments are often used to achieve this. Starting from perovskite precursors and usually additives (anti-solvent) dissolved in a suitable solvent, the assembly loaded in a printing cartridge is printed on a rigid or flexible substrate.

After drying to evaporate the solvents, a post-print heat treatment is performed to improve the quality of the crystallographic structure and the optoelectronic properties of the cell. The precision of the printing process minimises the consumption of raw materials, which are often toxic [112]. More and more non-toxic materials, such as solvents, are being incorporated through molecular engineering [114]. Chalkias et al. demonstrate for the first

time using such a low-molarity solvent, gamma-valerolactone (GVL), to fabricate a fully ambient printed PSC. GVL is a promising green alternative for preparing highly stable inkjet inks with over two months (1440 h) of storage without antisolvent or annealing [115]. Rubtsov et al. develop an effective strategy for inkjet fabrication of high-performance plasmonic architectures based on 2D arrays of TiO_2 microdots with integrated AuNPs and present the superior performance of the plasmon-enhanced PSC device [116].

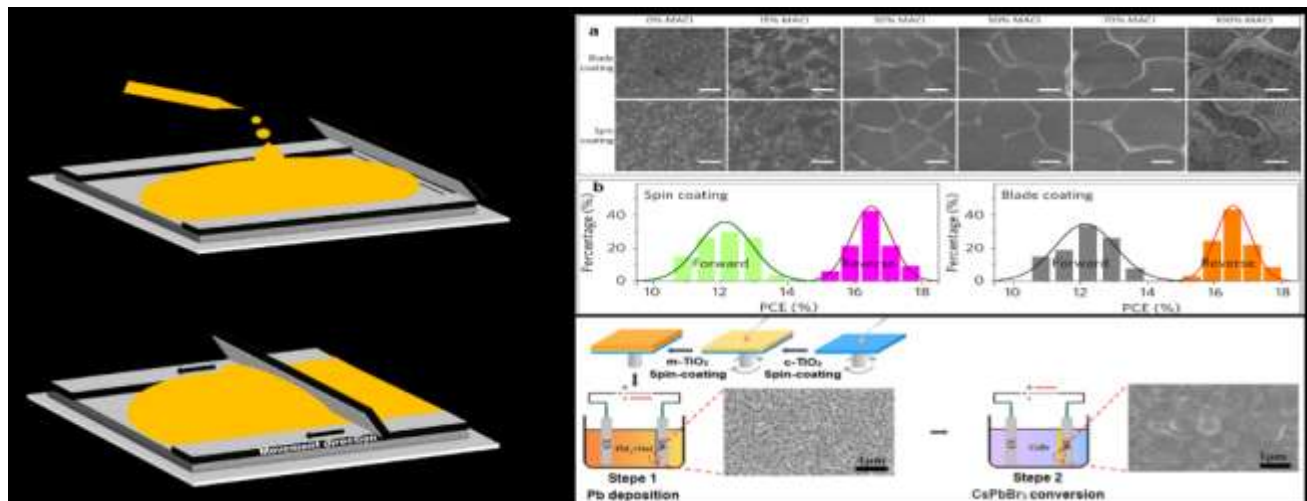


Fig. 3.I) Doctor blading: a) solution deposition, b) scraping; II) comparison between spin and the blade coating process: a) morphology, (b) PCEs [106]; III) illustration of the electrodeposition process: SEM monitoring of the various stages[110]

Conclusion:-

This review focused on the evolution of power conversion efficiency and stability since the appearance of this cell, the different families of PSCs and the elaboration techniques of a PSCs. The main findings of this study are as follows:

- From the first PSC to the most recent ones, progress has been presented in conversion efficiency and stability. PSCs have achieved an exceptional efficiency of 26.7% in 2024, only 0.6% away from the record set by silicon technology. This efficiency results from a significant research effort driven by the rapid progress facilitated by the exceptional optoelectronic properties of perovskite. Starting with DSSCs, perovskite has evolved thanks to advances in various aspects, including molecular engineering of precursors and solvents, interface and contact engineering. Growth control and nucleation, cell structure and processing techniques are just some of the aspects that have been explored, leading to some remarkable results recently. Difficulties such as toxicity, stability and scalability are increasingly being minimised. Recent advances in stability demonstrated by sustained performance ($\text{PCE} \geq 25\%$) for over 1000 hours and promising tests of mini-modules and modules, the long-awaited industrial production now appears imminent. Although lead, an essential perovskite component, is toxic, its impact remains controversial, given the quantities used. Research suggests that lead will continue to be widely used due to the large performance gap with perovskites using potential substituents, the most important of which is tin. In addition to the great efforts being made to improve the performance of tin-based cells, it is also necessary to address the issue of stability, which currently lags far behind that of lead perovskites.
- It turns out that progress in perovskites is mainly due to molecular engineering based on the basic structure of perovskite, which offers diverse family of perovskite materials, from simple to complex, by mixing. Three technologies in the perovskite family, including organometallic perovskites, inorganic perovskites, and perovskite nanocrystals, have been studied in detail. Organometallic perovskites were the first to be developed and the most advanced in efficiency. However, the difficulty of stabilising them has led to other technologies, including inorganic ones. Inorganic perovskites are more stable despite their low conversion efficiency. To overcome the stability problem and approach the theoretical limit, QDs have been the focus of intense research to control the optoelectronic properties of the cells better.
- The choice of processing techniques is crucial, both in terms of economics and efficiency. Spin coating is the most efficient technique, but it is limited by surface area, which is not an advantage for commercialisation. Record yields are only achieved in very small areas. In contrast, thermal evaporation allows deposition over

large areas. It also offers high-quality devices, but it's still very expensive. Dip coating is again essential for fibre cells, offering greater flexibility in fibre geometry. As a scalable technique, blading is showing promising results for large-scale production. Coupled with surfactant solvent engineering, control of crystallisation kinetics has greatly improved cell performance.

The various purification methods presented here represent only some of those in use. Spin-coating is the only non-scalable method, but it is essential to mention it since it is the most widely used in research. Rapid progress is being made for all the scalable techniques presented, but efforts must be made to achieve more efficient, less costly cells for commercialisation

Acknowledgments:-

The authors express their gratitude to the partner through the Support Project for the Reform of Science and Engineering Education (PARESI) and the associated laboratories.

Conflicts of Interest

The authors declare no conflicts of interest

References:-

1. Valsalakumar, S., Roy, A., Mallick, T.K., Hinshelwood, J., Sundaram, S.: An Overview of Current Printing Technologies for Large-Scale Perovskite Solar Cell Development. *Energies*. 16, 190 (2022)
2. Bati, A.S., Zhong, Y.L., Burn, P.L., Nazeeruddin, M.K., Shaw, P.E., Batmunkh, M.: Next-generation applications for integrated perovskite solar cells. *Communications Materials*. 4, 2 (2023)
3. Chen, Y., Zhang, M., Li, F., Yang, Z.: Recent Progress in Perovskite Solar Cells: Status and Future. *Coatings*. 13, 644 (2023)
4. Kojima, A., Teshima, K., Shirai, Y., Miyasaka, T.: Organometal halide perovskites as visible-light sensitizers for photovoltaic cells. *Journal of the American Chemical Society*. 131, 6050–6051 (2009)
5. Im, J.-H., Lee, C.-R., Lee, J.-W., Park, S.-W., Park, N.-G.: 6.5% efficient perovskite quantum-dot-sensitized solar cell. *Nanoscale*. 3, 4088–4093 (2011)
6. Chung, I., Lee, B., He, J., Chang, R.P., Kanatzidis, M.G.: All-solid-state dye-sensitized solar cells with high efficiency. *Nature*. 485, 486–489 (2012)
7. Kim, H.-S., Lee, C.-R., Im, J.-H., Lee, K.-B., Moehl, T., Marchioro, A., Moon, S.-J., Humphry-Baker, R., Yum, J.-H., Moser, J.E.: Lead iodide perovskite sensitized all-solid-state submicron thin film mesoscopic solar cell with efficiency exceeding 9%. *Scientific reports*. 2, 591 (2012)
8. Lee, M.M., Teucher, J., Miyasaka, T., Murakami, T.N., Snaith, H.J.: Efficient hybrid solar cells based on meso-superstructured organometal halide perovskites. *Science*. 338, 643–647 (2012)
9. Ball, J.M., Lee, M.M., Hey, A., Snaith, H.J.: Low-temperature processed meso-superstructured to thin-film perovskite solar cells. *Energy & Environmental Science*. 6, 1739–1743 (2013)
10. Liu, D., Kelly, T.L.: Perovskite solar cells with a planar heterojunction structure prepared using room-temperature solution processing techniques. *Nature photonics*. 8, 133–138 (2014)
11. Jeon, N.J., Noh, J.H., Kim, Y.C., Yang, W.S., Ryu, S., Seok, S.I.: Solvent engineering for high-performance inorganic–organic hybrid perovskite solar cells. *Nature materials*. 13, 897–903 (2014)
12. Saliba, M., Matsui, T., Domanski, K., Seo, J.-Y., Ummadisingu, A., Zakeeruddin, S.M., Correa-Baena, J.-P., Tress, W.R., Abate, A., Hagfeldt, A.: Incorporation of rubidium cations into perovskite solar cells improves photovoltaic performance. *Science*. 354, 206–209 (2016)
13. Burschka, J., Pellet, N., Moon, S.-J., Humphry-Baker, R., Gao, P., Nazeeruddin, M.K., Grätzel, M.: Sequential deposition as a route to high-performance perovskite-sensitized solar cells. *Nature*. 499, 316–319 (2013)
14. Chen, B., Rudd, P.N., Yang, S., Yuan, Y., Huang, J.: Imperfections and their passivation in halide perovskite solar cells. *Chemical Society Reviews*. 48, 3842–3867 (2019)
15. Liu, M., Johnston, M.B., Snaith, H.J.: Efficient planar heterojunction perovskite solar cells by vapour deposition. *Nature*. 501, 395–398 (2013)
16. Noh, J.H., Im, S.H., Heo, J.H., Mandal, T.N., Seok, S.I.: Chemical management for colorful, efficient, and stable inorganic–organic hybrid nanostructured solar cells. *Nano letters*. 13, 1764–1769 (2013)
17. Im, J.-H., Jang, I.-H., Pellet, N., Grätzel, M., Park, N.-G.: Growth of CH₃NH₃PbI₃ cuboids with controlled size for high-efficiency perovskite solar cells. *Nature nanotechnology*. 9, 927–932 (2014)
18. Zhou, H., Chen, Q., Li, G., Luo, S., Song, T., Duan, H.-S., Hong, Z., You, J., Liu, Y., Yang, Y.: Interface engineering of highly efficient perovskite solar cells. *Science*. 345, 542–546 (2014)

19. Yang, W.S., Noh, J.H., Jeon, N.J., Kim, Y.C., Ryu, S., Seo, J., Seok, S.I.: High-performance photovoltaic perovskite layers fabricated through intramolecular exchange. *Science*. 348, 1234–1237 (2015)
20. Jiang, Q., Chu, Z., Wang, P., Yang, X., Liu, H., Wang, Y., Yin, Z., Wu, J., Zhang, X., You, J.: Planar-structure perovskite solar cells with efficiency beyond 21%. *Advanced materials*. 29, 1703852 (2017)
21. Jung, E.H., Jeon, N.J., Park, E.Y., Moon, C.S., Shin, T.J., Yang, T.-Y., Noh, J.H., Seo, J.: Efficient, stable and scalable perovskite solar cells using poly (3-hexylthiophene). *Nature*. 567, 511–515 (2019)
22. Jeong, M., Choi, I.W., Go, E.M., Cho, Y., Kim, M., Lee, B., Jeong, S., Jo, Y., Choi, H.W., Lee, J., Bae, J.-H., Kwak, S.K., Kim, D.S., Yang, C.: Stable perovskite solar cells with efficiency exceeding 24.8% and 0.3-V voltage loss. *Science*. 369, 1615–1620 (2020). <https://doi.org/10.1126/science.abb7167>
23. Green, M.A., Dunlop, E.D., Yoshita, M., Kopidakis, N., Bothe, K., Siefert, G., Hinken, D., Rauer, M., Hohl-Ebinger, J., Hao, X.: Solar cell efficiency tables (Version 64). *Progress in photovoltaics: research and applications*. 32, 425–441 (2024)
24. Saliba, M., Matsui, T., Seo, J.-Y., Domanski, K., Correa-Baena, J.-P., Nazeeruddin, M.K., Zakeeruddin, S.M., Tress, W., Abate, A., Hagfeldt, A.: Cesium-containing triple cation perovskite solar cells: improved stability, reproducibility and high efficiency. *Energy & environmental science*. 9, 1989–1997 (2016)
25. Abuhelaiqa, M., Shibayama, N., Gao, X.-X., Kanda, H., Nazeeruddin, M.K.: SnO₂/TiO₂ electron transporting bilayers: a route to light stable perovskite solar cells. *ACS Applied Energy Materials*. 4, 3424–3430 (2021)
26. Tumen-Ulzii, G., Matsushima, T., Klotz, D., Leyden, M.R., Wang, P., Qin, C., Lee, J.-W., Lee, S.-J., Yang, Y., Adachi, C.: Hysteresis-less and stable perovskite solar cells with a self-assembled monolayer. *Communications Materials*. 1, 31 (2020)
27. Ren, Y., Zhang, K., Lin, Z., Wei, X., Xu, M., Huang, X., Chen, H., Yang, S.: Long-Chain Gemini Surfactant-Assisted Blade Coating Enables Large-Area Carbon-Based Perovskite Solar Modules with Record Performance. *Nano-Micro Letters*. 15, 182 (2023)
28. Lv, X., Gao, X., Yu, Z., Xiao, G.-B., Cao, J., Tang, Y.: One-pot surface and buried interface manipulation of perovskite film for efficient solar cells. *Cell Reports Physical Science*. 4, (2023)
29. Li, N., Niu, X., Li, L., Wang, H., Huang, Z., Zhang, Y., Chen, Y., Zhang, X., Zhu, C., Zai, H.: Liquid medium annealing for fabricating durable perovskite solar cells with improved reproducibility. *Science*. 373, 561–567 (2021)
30. Zhao, Y., Ma, F., Qu, Z., Yu, S., Shen, T., Deng, H.-X., Chu, X., Peng, X., Yuan, Y., Zhang, X.: Inactive (PbI₂) 2RbCl stabilizes perovskite films for efficient solar cells. *Science*. 377, 531–534 (2022)
31. Liang, L., Zhang, Z., Li, Y., Yu, X., Lin, F., Xu, Y., Lan, Z., Cavazzini, M., Pozzi, G., Orlandi, S.: Development of Pyr-TPA as Interfacial Passivation Layer Enabling Efficient and Stable n-i-p Perovskite Solar Cells. *Solar RRL*. 2300415
32. Wang, H., Qin, Z., Miao, Y., Zhao, Y.: Recent Progress in Large-Area Perovskite Photovoltaic Modules. *Transactions of Tianjin University*. 28, 323–340 (2022)
33. Abdollahi Nejand, B., Ritzer, D.B., Hu, H., Schackmar, F., Moghadamzadeh, S., Feeney, T., Singh, R., Laufer, F., Schmager, R., Azmi, R.: Scalable two-terminal all-perovskite tandem solar modules with a 19.1% efficiency. *Nature Energy*. 7, 620–630 (2022)
34. Lee, S.-W., Bae, S., Kim, D., Lee, H.-S.: Historical analysis of high-efficiency, large-area solar cells: toward upscaling of perovskite solar cells. *Advanced Materials*. 32, 2002202 (2020)
35. Chen, S., Dai, X., Xu, S., Jiao, H., Zhao, L., Huang, J.: Stabilizing perovskite-substrate interfaces for high-performance perovskite modules. *Science*. 373, 902–907 (2021)
36. Pescetelli, S., Agresti, A., Viskadourous, G., Razza, S., Rogdakis, K., Kalogerakis, I., Spiliarotis, E., Leonardi, E., Mariani, P., Sorbello, L.: Integration of two-dimensional materials-based perovskite solar panels into a stand-alone solar farm. *Nature Energy*. 7, 597–607 (2022)
37. Solar cell efficiency tables (Version 64), <https://onlinelibrary.wiley.com/doi/abs/10.1002/pip.3831>, (2024)
38. Rezaee, E., Kutsarov, D., Li, B., Bi, J., Silva, S.R.P.: A route towards the fabrication of large-scale and high-quality perovskite films for optoelectronic devices. *Scientific reports*. 12, 7411 (2022)
39. Dawa, T., Sajjadi, B.: Exploring the potential of perovskite structures for chemical looping technology: A state-of-the-art review. *Fuel Processing Technology*. 253, 108022 (2024). <https://doi.org/10.1016/j.fuproc.2023.108022>
40. Chakraborty, K., Choudhury, M.G., Paul, S.: Study of physical, optical, and electrical properties of cesium titanium (IV)-based single halide perovskite solar cell. *IEEE Journal of Photovoltaics*. 11, 386–390 (2021)
41. Yandri, V.R., Nurunnizar, A.A., Debora, R., Wulandari, P., Nursam, N.M., Hidayat, R., Indari, E.D., Yamashita, Y.: Crystal structures and photoluminescence characteristics of cesium lead bromide perovskite nanoplatelets depending on the antisolvent and ligand used in their syntheses. *Heliyon*. 10, (2024)

42. Gómez-Toledo, M., Boulahya, K., Collado, L., Arroyo-de Dompablo, M.E.: Upgrading photocatalytic hydrogen evolution in Ba–Sr–Ta–O perovskite-type layered structures. *International Journal of Hydrogen Energy*. 63, 1003–1012 (2024)
43. Mohammadi, A., Thurner, C.W., Haug, L., Bekheet, M.F., Müller, J.T., Gurlo, A., Hejny, C., Nezhad, P.D.K., Winkler, D., Riedel, W.: How defects in lanthanum iron manganite perovskite structures promote the catalytic reduction of NO by CO. *Materials Today Chemistry*. 35, 101910 (2024)
44. Assirey, E.A.R.: Perovskite synthesis, properties and their related biochemical and industrial application. *Saudi Pharmaceutical Journal*. 27, 817–829 (2019)
45. Thomson, S.: Observing phase transitions in a halide perovskite using temperature dependent photoluminescence spectroscopy. Livingston: Edinburgh Instruments, AN_P45. (2018)
46. Zhao, Y., Xiang, H., Ran, R., Zhou, W., Wang, W., Shao, Z.: Beyond two-dimension: One- and zero-dimensional halide perovskites as new-generation passivators for high-performance perovskite solar cells. *Journal of Energy Chemistry*. 83, 189–208 (2023). <https://doi.org/10.1016/j.jechem.2023.04.025>
47. Liu, X., Cao, L., Guo, Z., Li, Y., Gao, W., Zhou, L.: A review of perovskite photovoltaic materials' synthesis and applications via chemical vapor deposition method. *Materials*. 12, 3304 (2019)
48. Wang, Y., Zhang, Y., Zhang, P., Zhang, W.: High intrinsic carrier mobility and photon absorption in the perovskite CH₃NH₃PbI₃. *Physical Chemistry Chemical Physics*. 17, 11516–11520 (2015)
49. Meng, X., Wang, Y., Lin, J., Liu, X., He, X., Barbaud, J., Wu, T., Noda, T., Yang, X., Han, L.: Surface-Controlled Oriented Growth of FASnI₃ Crystals for Efficient Lead-free Perovskite Solar Cells. *Joule*. 4, 902–912 (2020). <https://doi.org/10.1016/j.joule.2020.03.007>
50. Zhu, Z., Jiang, X., Yu, D., Yu, N., Ning, Z., Mi, Q.: Smooth and compact FASnI₃ films for lead-free perovskite solar cells with over 14% efficiency. *ACS Energy Letters*. 7, 2079–2083 (2022)
51. Wang, Y.-D., Wang, Y., Shao, J.-Y., Lan, Y., Lan, Z.-R., Zhong, Y.-W., Song, Y.: Defect Passivation by a D–A–D Type Hole-Transporting Interfacial Layer for Efficient and Stable Perovskite Solar Cells. *ACS Energy Letters*. 6, 2030–2037 (2021)
52. Yang, D., Zhang, X., Wang, K., Wu, C., Yang, R., Hou, Y., Jiang, Y., Liu, S., Priya, S.: Stable efficiency exceeding 20.6% for inverted perovskite solar cells through polymer-optimized PCBM electron-transport layers. *Nano letters*. 19, 3313–3320 (2019)
53. Liu, S., Zhang, D., Sheng, Y., Zhang, W., Qin, Z., Qin, M., Li, S., Wang, Y., Gao, C., Wang, Q., Ming, Y., Liu, C., Yang, K., Huang, Q., Qi, J., Gao, Q., Chen, K., Hu, Y., Rong, Y., Lu, X., Mei, A., Han, H.: Highly oriented MAPbI₃ crystals for efficient hole-conductor-free printable mesoscopic perovskite solar cells. *Fundamental Research*. 2, 276–283 (2022). <https://doi.org/10.1016/j.fmre.2021.09.008>
54. Fateev, S.A., Petrov, A.A., Khrustalev, V.N., Dorovatovskii, P.V., Zubavichus, Y.V., Goodilin, E.A., Tarasov, A.B.: Solution Processing of Methylammonium Lead Iodide Perovskite from γ -Butyrolactone: Crystallization Mediated by Solvation Equilibrium. *Chem. Mater*. 30, 5237–5244 (2018). <https://doi.org/10.1021/acs.chemmater.8b01906>
55. Jeong, J., Kim, M., Seo, J., Lu, H., Ahlawat, P., Mishra, A., Yang, Y., Hope, M.A., Eickemeyer, F.T., Kim, M.: Pseudo-halide anion engineering for α -FAPbI₃ perovskite solar cells. *Nature*. 592, 381–385 (2021)
56. Lu, H., Liu, Y., Ahlawat, P., Mishra, A., Tress, W.R., Eickemeyer, F.T., Yang, Y., Fu, F., Wang, Z., Avalos, C.E.: Vapor-assisted deposition of highly efficient, stable black-phase FAPbI₃ perovskite solar cells. *Science*. 370, eabb8985 (2020)
57. Min, H., Kim, M., Lee, S.-U., Kim, H., Kim, G., Choi, K., Lee, J.H., Seok, S.I.: Efficient, stable solar cells by using inherent bandgap of α -phase formamidinium lead iodide. *Science*. 366, 749–753 (2019)
58. Lyu, M., Park, N.-G.: Effect of additives AX (A= FA, MA, Cs, Rb, NH₄, X= Cl, Br, I) in FAPbI₃ on photovoltaic parameters of perovskite solar cells. *Solar RRL*. 4, 2000331 (2020)
59. Yue, X., Wang, C., Zhang, B., Zhang, Z., Xiong, Z., Zu, X., Liu, Z., Hu, Z., Odunmbaku, G.O., Zheng, Y.: Real-time observation of the buildup of polaron in α -FAPbI₃. *Nature Communications*. 14, 917 (2023)
60. Li, G., Su, Z., Canil, L., Hughes, D., Aldamasy, M.H., Dagar, J., Trofimov, S., Wang, L., Zuo, W., Jerónimo-Rendon, J.J.: Highly efficient pin perovskite solar cells that endure temperature variations. *Science*. 379, 399–403 (2023)
61. Liang, J., Wang, C., Wang, Y., Xu, Z., Lu, Z., Ma, Y., Zhu, H., Hu, Y., Xiao, C., Yi, X., Zhu, G., Lv, H., Ma, L., Chen, T., Tie, Z., Jin, Z., Liu, J.: All-Inorganic Perovskite Solar Cells. *J. Am. Chem. Soc*. 138, 15829–15832 (2016). <https://doi.org/10.1021/jacs.6b10227>
62. Eze, V.O., Carani, L.B., Majumder, H., Uddin, M.J., Okoli, O.I.: Inorganic cesium lead mixed halide based perovskite solar materials modified with functional silver iodide. *Scientific reports*. 12, 1–10 (2022)

63. Wang, Y., Chen, Y., Zhang, T., Wang, X., Zhao, Y.: Chemically Stable Black Phase CsPbI₃ Inorganic Perovskites for High-Efficiency Photovoltaics. *Advanced Materials*. 32, 2001025 (2020)
64. Choi, H., Jeong, J., Kim, H.-B., Kim, S., Walker, B., Kim, G.-H., Kim, J.Y.: Cesium-doped methylammonium lead iodide perovskite light absorber for hybrid solar cells. *Nano Energy*. 7, 80–85 (2014)
65. Eperon, G.E., Paternò, G.M., Sutton, R.J., Zampetti, A., Haghighirad, A.A., Cacialli, F., Snaith, H.J.: Inorganic caesium lead iodide perovskite solar cells. *Journal of Materials Chemistry A*. 3, 19688–19695 (2015)
66. Noel, N.K., Congiu, M., Ramadan, A.J., Fearn, S., McMeekin, D.P., Patel, J.B., Johnston, M.B., Wenger, B., Snaith, H.J.: Unveiling the Influence of pH on the Crystallization of Hybrid Perovskites, Delivering Low Voltage Loss Photovoltaics. *Joule*. 1, 328–343 (2017). <https://doi.org/10.1016/j.joule.2017.09.009>
67. Ke, W., Spanopoulos, I., Stoumpos, C.C., Kanatzidis, M.G.: Myths and reality of HPbI₃ in halide perovskite solar cells. *Nature communications*. 9, 4785 (2018)
68. Pei, Y., Liu, Y., Li, F., Bai, S., Jian, X., Liu, M.: Unveiling property of hydrolysis-derived DMAPbI₃ for perovskite devices: composition engineering, defect mitigation, and stability optimization. *Iscience*. 15, 165–172 (2019)
69. Wang, Y., Liu, X., Zhang, T., Wang, X., Kan, M., Shi, J., Zhao, Y.: The role of dimethylammonium iodide in CsPbI₃ perovskite fabrication: additive or dopant? *Angewandte Chemie*. 131, 16844–16849 (2019)
70. Cui, Y., Shi, J., Meng, F., Yu, B., Tan, S., He, S., Tan, C., Li, Y., Wu, H., Luo, Y.: A Versatile Molten-Salt Induction Strategy to Achieve Efficient CsPbI₃ Perovskite Solar Cells with a High Open-Circuit Voltage > 1.2 V. *Advanced Materials*. 34, 2205028 (2022)
71. Zhang, J., Wang, Z., Mishra, A., Yu, M., Shasti, M., Tress, W., Kubicki, D.J., Avalos, C.E., Lu, H., Liu, Y.: Intermediate phase enhances inorganic perovskite and metal oxide interface for efficient photovoltaics. *Joule*. 4, 222–234 (2020)
72. Ye, Q., Ma, F., Zhao, Y., Yu, S., Chu, Z., Gao, P., Zhang, X., You, J.: Stabilizing γ -CsPbI₃ Perovskite via Phenylethylammonium for Efficient Solar Cells with Open-Circuit Voltage over 1.3 V. *Small*. 16, 2005246 (2020)
73. Fatima, K., Haider, M.I., Bashir, A., Qamar, S., Qureshi, A.A., Akhter, Z., Sultan, M.: Surface modification of CsPbI₂Br for improved performance of inorganic perovskite solar cells. *Physica E: Low-dimensional Systems and Nanostructures*. 142, 115265 (2022)
74. Kang, Y., Kang, S., Han, S.: Influence of Bi doping on physical properties of lead halide perovskites: a comparative first-principles study between CsPbI₃ and CsPbBr₃. *Materials Today Advances*. 3, 100019 (2019)
75. Li, X., Wang, K., Lgbari, F., Dong, C., Yang, W., Ma, C., Ma, H., Wang, Z.-K., Liao, L.-S.: Indium doped CsPbI₃ films for inorganic perovskite solar cells with efficiency exceeding 17%. *Nano Research*. 13, 2203–2208 (2020)
76. Khan, J., Ullah, I., Yuan, J.: CsPbI₃ perovskite quantum dot solar cells: opportunities, progress and challenges. *Materials Advances*. 3, 1931–1952 (2022)
77. Schaller, R.D., Klimov, V.I.: High efficiency carrier multiplication in PbSe nanocrystals: implications for solar energy conversion. *Physical review letters*. 92, 186601 (2004)
78. Jia, D., Chen, J., Qiu, J., Ma, H., Yu, M., Liu, J., Zhang, X.: Tailoring solvent-mediated ligand exchange for CsPbI₃ perovskite quantum dot solar cells with efficiency exceeding 16.5%. *Joule*. 6, 1632–1653 (2022)
79. Dally, P.: Characterization of perovskite systems: understanding and improving the performance and stability of photovoltaic devices. *Universite de Grenoble Alpes* (2019)
80. Bouchard, M., Hilhorst, J., Pouget, S., Alam, F., Mendez, M., Djurado, D., Aldakov, D., Schüllli, T., Reiss, P.: Direct evidence of chlorine-induced preferential crystalline orientation in methylammonium lead iodide perovskites grown on TiO₂. *The Journal of Physical Chemistry C*. 121, 7596–7602 (2017)
81. Singh, T., Miyasaka, T.: Stabilizing the efficiency beyond 20% with a mixed cation perovskite solar cell fabricated in ambient air under controlled humidity. *Advanced Energy Materials*. 8, 1700677 (2018)
82. Adnan, M., Irshad, Z., Lee, J.K.: Facile all-dip-coating deposition of highly efficient (CH₃)₃NPbI₃-xCl_x perovskite materials from aqueous non-halide lead precursor. *RSC Adv*. 10, 29010–29017 (2020). <https://doi.org/10.1039/D0RA06074G>
83. Li, H., Zhou, J., Tan, L., Li, M., Jiang, C., Wang, S., Zhao, X., Liu, Y., Zhang, Y., Ye, Y., Tress, W., Yi, C.: Sequential vacuum-evaporated perovskite solar cells with more than 24% efficiency, (2022)
84. Bae, S.-R., Heo, D.Y., Kim, S.Y.: Recent progress of perovskite devices fabricated using thermal evaporation method: Perspective and outlook. *Materials Today Advances*. 14, 100232 (2022)
85. Ye, Y., Jiao, B., Li, M., Tan, L., Zhao, J., Li, H., Ren, N., Su, R., Prochowicz, D., Liu, Y.: Vacuum-Evaporated Perovskite and Interfacial Modifier for Efficient Perovskite Solar Cells. *Small*. 21, 2501410 (2025)

86. Li, X., Tan, Y., Lai, H., Li, S., Chen, Y., Li, S., Xu, P., Yang, J.: All-inorganic CsPbBr₃ perovskite solar cells with 10.45% efficiency by evaporation-assisted deposition and setting intermediate energy levels. *ACS Applied materials & interfaces*. 11, 29746–29752 (2019)
87. Farag, A., Feeney, T., Hossain, I.M., Schackmar, F., Fassl, P., Küster, K., Bäuerle, R., Ruiz-Preciado, M.A., Hentschel, M., Ritzer, D.B.: Evaporated Self-Assembled Monolayer Hole Transport Layers: Lossless Interfaces in p-i-n Perovskite Solar Cells. *Advanced Energy Materials*. 13, 2203982 (2023)
88. Cherrington, R., Liang, J.: Materials and deposition processes for multifunctionality. *Design and Manufacture of Plastic Components for Multifunctionality: Structural Composites, Injection Molding, and 3D Printing*. 19–21 (2016)
89. Adnan, M., Lee, J.K.: Highly efficient planar heterojunction perovskite solar cells with sequentially dip-coated deposited perovskite layers from a non-halide aqueous lead precursor. *RSC Adv*. 10, 5454–5461 (2020). <https://doi.org/10.1039/C9RA09607H>
90. Froehlich, M.: Two coating problems: Thin film rupture and spin coating, (2009)
91. Sahu, N., Parija, B., Panigrahi, S.: Fundamental understanding and modeling of spin coating process: A review. *Indian Journal of Physics*. 83, 493–502 (2009)
92. Shaikh, J.S., Shaikh, N.S., Sheikh, A.D., Mali, S.S., Kale, A.J., Kanjanaboos, P., Hong, C.K., Kim, J.H., Patil, P.S.: Perovskite solar cells: In pursuit of efficiency and stability. *Materials & Design*. 136, 54–80 (2017)
93. Lee, J.-W., Park, N.-G.: Two-step deposition method for high-efficiency perovskite solar cells. *MRS Bulletin*. 40, 654–659 (2015). <https://doi.org/10.1557/mrs.2015.166>
94. Butt, M.A.: Thin-film coating methods: A successful marriage of high-quality and cost-effectiveness—A brief exploration. *Coatings*. 12, 1115 (2022)
95. Butt, M.A.: Thin-film coating methods: A successful marriage of high-quality and cost-effectiveness—A brief exploration. *Coatings*. 12, 1115 (2022)
96. Lalpour, N., Mirkhani, V., Keshavarzi, R., Moghadam, M., Tangestaninejad, S., Mohammadpoor-Baltork, I., Gao, P.: Self-healing perovskite solar cells based on copolymer-templated TiO₂ electron transport layer. *Scientific Reports*. 13, 6368 (2023)
97. Adnan, M., Lee, J.K.: All sequential dip-coating processed perovskite layers from an aqueous lead precursor for high efficiency perovskite solar cells. *Scientific reports*. 8, 2168 (2018)
98. Lv, D., Jiang, Q., Shang, Y., Liu, D.: Highly efficient fiber-shaped organic solar cells toward wearable flexible electronics. *npj Flexible Electronics*. 6, 38 (2022)
99. Li, F., Zhang, Y., Jiang, K.-J., Zhang, C., Huang, J.-H., Wang, H., Fan, H., Wang, P., Chen, Y., Zhao, W.: A Novel Strategy for Scalable High-Efficiency Planar Perovskite Solar Cells with New Precursors and Cation Displacement Approach. *Advanced Materials*. 30, 1804454 (2018)
100. Hong, S., Han, A., Lee, E.C., Ko, K.-W., Park, J.-H., Song, H.-J., Han, M.-H., Han, C.-H.: A facile and low-cost fabrication of TiO₂ compact layer for efficient perovskite solar cells. *Current Applied Physics*. 15, 574–579 (2015)
101. Hong, S., Han, A., Lee, E.C., Ko, K.-W., Park, J.-H., Song, H.-J., Han, M.-H., Han, C.-H.: A facile and low-cost fabrication of TiO₂ compact layer for efficient perovskite solar cells. *Current Applied Physics*. 15, 574–579 (2015)
102. Rahman, K.M., Amiri, O., Younis, K.A., Khalil, M.H., Azhdarpour, A.M., Saadat, M., Jamal, M.A., Abdulrahman, N.A., Ismael, S.J., Ibrahim, K.A.: Stable perovskite solar cells resist to water without encapsulation by p-type Si NWs as hole collection layers. *Journal of Nanostructures*. (2023)
103. Masood, M.T., Weinberger, C., Sarfraz, J., Rosqvist, E., Sandén, S., Sandberg, O.J., Vivo, P., Hashmi, G., Lund, P.D., Osterbacka, R.: Impact of film thickness of ultrathin dip-coated compact TiO₂ layers on the performance of mesoscopic perovskite solar cells. *ACS applied materials & interfaces*. 9, 17906–17913 (2017)
104. Wu, W.-Q., Wang, Q., Fang, Y., Shao, Y., Tang, S., Deng, Y., Lu, H., Liu, Y., Li, T., Yang, Z.: Molecular doping enabled scalable blading of efficient hole-transport-layer-free perovskite solar cells. *Nature communications*. 9, 1–8 (2018)
105. Li, Z., Klein, T.R., Kim, D.H., Yang, M., Berry, J.J., Van Hest, M.F., Zhu, K.: Scalable fabrication of perovskite solar cells. *Nature Reviews Materials*. 3, 1–20 (2018)
106. Yang, M., Li, Z., Reese, M.O., Reid, O.G., Kim, D.H., Siol, S., Klein, T.R., Yan, Y., Berry, J.J., Van Hest, M.F.: Perovskite ink with wide processing window for scalable high-efficiency solar cells. *Nature Energy*. 2, 1–9 (2017)
107. Peng, Y., Cheng, Y., Wang, C., Zhang, C., Xia, H., Huang, K., Tong, S., Hao, X., Yang, J.: Fully doctor-bladed planar heterojunction perovskite solar cells under ambient condition. *Organic Electronics*. 58, 153–158 (2018). <https://doi.org/10.1016/j.orgel.2018.04.020>

108. Chang, J., Feng, E., Li, H., Ding, Y., Long, C., Gao, Y., Yang, Y., Yi, C., Zheng, Z., Yang, J.: Crystallization and Orientation Modulation Enable Highly Efficient Doctor-Bladed Perovskite Solar Cells. *Nano-Micro Letters*. 15, 164 (2023)
109. Al Katrib, M., Perrin, L., Planes, E.: A Way to Reach 10% Efficiency with Carbon-Based Electrodeposited Mixed Perovskite Solar Cells. *Solar RRL*. 6, 2200777 (2022)
110. Wang, X., Abbasi, S., Zhang, D., Wang, J., Wang, Y., Cheng, Z., Liu, H., Shen, W.: Electrochemical deposition of CsPbBr₃ perovskite for photovoltaic devices with robust ambient stability. *ACS Applied Materials & Interfaces*. 12, 50455–50463 (2020)
111. Lv, P., Zhang, P., Chen, Z., Dong, S., Liu, M., Ma, J., Cai, J., Sun, F., Li, S.: The preparation of all-inorganic CsPbI₂-xBr_{1+x} perovskite solar cells based on electrodeposited PbO₂ film. *Solar Energy*. 207, 618–625 (2020)
112. Cheng, Y., Wu, H., Ma, J., Li, P., Gu, Z., Zang, S., Han, L., Zhang, Y., Song, Y.: Droplet manipulation and crystallization regulation in inkjet-printed perovskite film formation. *CCS Chemistry*. 4, 1465–1485 (2022)
113. Maisch, P., Tam, K.C., Jang, D., Steinberger, M., Yang, F., Brabec, C.J., Egelhaaf, H.-J.: 10 - Inkjet printed organic and perovskite photovoltaics—review and perspectives. In: Cosseddu, P. and Caironi, M. (eds.) *Organic Flexible Electronics*. pp. 305–333. Woodhead Publishing (2021)
114. Kwon, N., Lee, J., Ko, M.J., Kim, Y.Y., Seo, J.: Recent progress of eco-friendly manufacturing process of efficient perovskite solar cells. *Nano Convergence*. 10, 1–18 (2023)
115. Chalkias, D.A., Mourtzikou, A., Katsagounos, G., Kalarakis, A.N., Stathatos, E.: Development of Greener and Stable Inkjet-Printable Perovskite Precursor Inks for All-Printed Annealing-Free Perovskite Solar Mini-Modules Manufacturing. *Small Methods*. 7, 2300664 (2023)
116. Rubtsov, S., Musin, A., Danchuk, V., Shatalov, M., Prasad, N., Zinigrad, M., Yadgarov, L.: Plasmon-Enhanced Perovskite Solar Cells Based on Inkjet-Printed Au Nanoparticles Embedded into TiO₂ Microdot Arrays. *Nanomaterials*. 13, 2675 (2023)